Available online at www.sciencedirect.com
SCIENCE DIRECT®
Journal of Theoretical Biology 238 (2006) 146–156
Journal of Theoretical Biology
www.elsevier.com/locate/yjtbi

Evolutionary game theory in an agent-based brain tumor model: Exploring the 'Genotype–Phenotype' link

Yuri Mansury[a,b], Mark Diggory[c], Thomas S. Deisboeck[a,b,*]

[a]*Complex Biosystems Modeling Laboratory, HST-Biomedical Engineering Center, Massachusetts Institute of Technology, Cambridge, MA 02139, USA*
[b]*Harvard-MIT (HST), Athinoula A. Martinos Center for Biomedical Imaging, Massachusetts General Hospital, Charlestown, MA 02129, USA*
[c]*Harvard-MIT Data Centre, Harvard University, Cambridge, MA 02138, USA*

Received 9 February 2005; accepted 4 May 2005
Available online 2 August 2005

Abstract

To investigate the genotype–phenotype link in a polyclonal cancer cell population, here we introduce evolutionary game theory into our previously developed agent-based brain tumor model. We model the heterogeneous cell population as a mixture of two distinct genotypes: the more proliferative Type A and the more migratory Type B. Our agent-based simulations reveal a phase transition in the tumor's velocity of spatial expansion linking the tumor fitness to genotypic composition. Specifically, velocity initially falls as rising payoffs reward the interactions among the more stationary Type A cells, but unexpectedly accelerates again when these A–A payoffs increase even further. At this latter accelerating stage, fewer migratory Type B cells appear to confer a competitive advantage in terms of the tumor's spatial aggression over the overall numerically dominating Type A cells, which in turn leads to an acceleration of the overall tumor dynamics while its surface roughness declines. We discuss potential implications of our findings for cancer research.

Keywords: Gliomas; Game theory; Agent based; Tumor modeling

1. Introduction

This manuscript proposes a game-theory framework to extend our previously developed spatio-temporal agent-based model of brain tumor cells (Mansury and Deisboeck 2003, 2004). In addition to rapid tissue invasion (Giese et al., 1996), these neoplasms are characterized by extensive heterogeneity (Shapiro, 1986), which contributes to the failure of current treatment modalities. Since integrating a game-theory module allows the modeling of cell–cell interactions in a polyclonal population of tumor cells, this step is, from a tumor biology perspective, a logical extension from our previously 'monoclonal' model that focused on phenotypic alterations. In particular, here we have a heterogenous population of tumor cells with two subpopulations that can be distinguished based on their distinct genotypes. The interactions among tumor cells and between cells and environment create the diametrically opposing forces of cooperation and competition, which can lead to nonlinear dynamics and complex spatial pattern. Cooperation emerges when a group of tumor cells together generate a synergistic effect in the form of higher fitness levels than those of individually isolated cells. At the same time, however, these cells also spatially compete with each other to occupy more permissive locations characterized by nutrient abundance. The discreteness of our agent-based model, where the smallest unit of observation is an individual tumor cell, naturally complements a game-theory module. Such a module focuses on pairwise cell–cell interactions, which require a spatially explicit model because they

*Corresponding author. Complex Biosystems Modeling Laboratory, Harvard-MIT (HST) Athinoula A. Martinos Center for Biomedical Imaging, Massachusetts General Hospital-East, Rm. 2301, Bldg. 149, 13th Street, Charlestown, MA 02129, USA. Tel.: +1 617 724 1845; fax: +1 617 726 5079
E-mail address: deisboec@helix.mgh.harvard.edu (T.S. Deisboeck).

0022-5193/$ - see front matter © 2005 Elsevier Ltd. All rights reserved.
doi:10.1016/j.jtbi.2005.05.027

lead to insightful complex dynamics that cease to exist in a non-spatial paradigm (Sole and Bascompte, 1992; Gonzalez-Garcia et al., 2002). Additionally, a temporal framework is necessary when the long-term outcome likely does not settle into Nash equilibrium[1] (Nowak and Sigmund, 1989; Nowak and May, 1995), which often happens when the current outcome depends dynamically on the previous frequency distribution, i.e. the relative proportions of the existing genotypes[2] in the tumor cell population.

'Game theory' originated within the field of social sciences in an effort to deal with the problem of interdependencies among interacting agents. Evolutionary biologists (e.g. Hamilton, 1967; Smith and Price, 1973) subsequently adopted the game-theory framework to model local cell–cell interactions. Since then, the number of papers that employ game theory to examine biological problems is in thousands (see Dugatkin and Reeve, 1998). The fundamental principal is that the actions of one individual have an impact on the 'fitness' of others, which in turn affect the evolutionary dynamics of the entire system. In the context of tumors, 'players' in a game-theory framework correspond to cells whose phenotypic behavior depends on both the genotypes of the cells they interact with (i.e., their 'co-players') and the microenvironment they face. Incorporating a game-theory framework is useful in a model that examines the feedback effects between tumors and their environment (Nowak and Sigmund, 2004). Experimentally, Roskelley and Bissel (2002) identified microenvironmental factors that can trigger genetic abnormalities, hence promoting the emergence of breast and ovarian cancer. Simulations have also shown that the relative frequencies of distinct genotypes in the tumor cell population depend on the environment (Kansal et al., 2001). This causal mechanism, however, captures only one-half of the evolutionary dynamics. The feedback loop closes when the environment itself adapts as a result of the changing population configuration.

A novel contribution of our paper is the explicit link between the genotypes of individual cells and their expressed phenotypical behavior. Previous evolutionary game-theory studies have been formulated exclusively in terms of phenotypes (Nowak and Sigmund, 2004), thereby ignoring the complexity of the *genotype–phenotype* link. The neglect is due to the lack of experimental evidence mapping 'allele' space to a 'trait' space. Our simulation model thus provides the starting point for exploring such a genotype–phenotype relationship and for hypotheses testing as more data become available in the future.

In the following, we briefly review previous works that specifically employ game-theoretic approaches to model local interactions in a heterogeneous population of cancer cells.

2. Previous studies

To our knowledge, Tomlinson (1997) first proposed a game-theory model of interacting tumor cells. However, he defines the strategy space based only on the production rates of cytotoxic metabolites that a tumor cell produces. This work focuses entirely on the cell–cell interactions between different genotypes of cancer cells and does not account for the interactions between cancer cells and the surrounding environment. In related work, Tomlinson and Bodmer (1997) developed a game-theory model of a cancer cell population consisting of two types of cells. They show that polymorphism (i.e. stable coexistence of two distinct genotypes) emerges if the benefits of angiogenesis are greater than the costs. Their model is continuous and non-spatial, but again they do not consider the interactions between cancer cells and their environment. More recently, Bach et al. (2001) introduced an agglomeration effect into Tomlinson and Bodmer's (1997) game-theory model of interacting tumor cells. Specifically, the authors assume that at any given time a cell can interact with up to two local neighbors. To gain a proliferative advantage, at least one of the cell's neighbors must be of the same genotype. Although their model is inspired by the impact of spatial heterogeneity, they do not explicitly propose a spatial model, nor do they consider the interplay between the cells and the environment. Conversely, Gatenby and Vincent (2003a) explicitly consider the cell–environment interactions in their game-theory model of colorectal carcinogenesis. Their work specifies that cells proliferate only if nutrient uptake exceeds the threshold metabolic requirements. These authors use a system of augmented Lotka–Volterra equations to convert nutrient uptake into new daughter cells. In a parallel work, Gatenby and Vincent (2003b) propose game-theoretic interactions between tumor and normal cells to examine the efficacy of various therapeutic strategies. In this line of Gatenby's works there is no geography in the model. In their previous work, Gatenby and Gawlinski (1996) and Gonzalez-Garcia et al. (2002) introduced spatial competition by adding a diffusion term to the system of Lotka–Volterra equations. Taken together, such continuum spatial models are most useful to model relatively large tumors consisting of a sizeable population of cells. However, a continuum approach may not

[1]Nash equilibrium in this context here corresponds to a set of genotypes with the property that no group of monoclonal cells can benefit (i.e. obtaining higher average fitness payoffs as a group) by altering the genotype of their offspring, e.g. through mutation. The set of such genotypes and the corresponding payoffs constitute the Nash Equilibrium.

[2]*Genotypes* here refer to the (fixed) genetic constitution of a tumor cell, which is distinct from the cell's expressed behavioral 'traits', or *phenotypes*, that can alternate.

be suitable during the crucial early stages of tumorigenesis characterized by a small, discrete number of tumor cells. Yet, from a systems perspective, it is arguably the spatio-temporal behavior of this initially relatively small number of tumor cells that subsequently establishes the evolutionary trajectory of the tumor (see, e.g. Mansury and Deisboeck, 2003, 2004). Specifically, the tumor's average spatial velocity determines how quickly cancer cells invade their surrounding brain parenchyma, which in turn often determines the patient's prognosis.

The following section details the game-theory module extending our previously developed agent-based model of malignant brain cancer (Mansury and Deisboeck, 2003, 2004). As in our previous works, we also hypothesize here that migrating tumor cells[3] are biased random walkers guided by the presence of environmental stimuli when they invade the (virtual) brain parenchyma. However, here we choose to include only nutrient gradients as the pertinent environmental factors while excluding toxic metabolites and mechanical confinements. Such a simplified setup allows us to establish the cause–effect link between the tumor and its microenvironment more transparently.

3. Model

3.1. Game-theory module

'Strategic' interactions among virtual cancer cells can be represented by a simple model of evolutionary game theory. Such a framework means that an interaction between two cells confers certain 'payoffs' whose specific value depends on the genotypes of the interacting cancer cells. In turn, these payoffs determine the cells' phenotypic behavior, thus completing the genotype–phenotype mapping. Here we will consider *local* interactions only: a cancer cell can interact only with its neighbor cells located in an adjacent location one lattice site away sharing a common border.

The game-theory features of our model are as follows: Initially at time $t = 0$ there are two equal-size subpopulations of cancer cells that can be distinguished based on their genotypes: A and B. We assume that the genetic makeups, resulting from mutational events, are such that genotype A is highly proliferative and exhibits higher inclination to communicate with other cells via gap junctions, while genotype B is highly migratory and performs lesser gap junction communications (see Table 1). We emphasize here that genotype A can also migrate (and genotype B can also proliferate); however, under the same environmental conditions genotype A has higher probability to proliferate than genotype B (while genotype B has higher probability to migrate). For now, neglecting further mutational events, these genotypes are fixed properties that never change during the lifetime of these virtual tumor cells.

Table 1
The distinctions between genotypes A and B in terms of their genetically encoded capability to proliferate, migrate, and communicate with other cells via gap junctions

	Genetic composition
Type A	Highly proliferative genotype High number of gap junctions
Type B	Highly migratory genotype Low number of gap junctions

Given the two genotypes, there are thus three possible pairs of interacting cells, namely A–A, A–B, and B–B. Let $N = \{1, 2, \ldots, n\}$ be the set of all viable cells in the population, which can be broken down into $n_{\mathrm{A},t}$ cells of Type A and $n_{\mathrm{B},t}$ cells of Type B, $n_{\mathrm{A}} + n_{\mathrm{B}} = n$. The relative proportions (i.e. *frequencies*) of these distinct genotypes in the total population are therefore $f_A = n_A/n$ and $f_B = 1 - f_A$ for Type A and B, respectively. When a pair of cells interacts, each cell is rewarded with certain 'payoffs', which affect their phenotypic behavior in terms of growth or migratory activities. In contrast to genotypic composition, phenotypic behavior can alter depending on the cell's partner of interaction and on the environmental factors. A payoff matrix summarizes the rewards for cell interactions affecting their phenotypes, but whose magnitude depends on the genotypes of the interacting cells, thus establishing the genotype–phenotype link.

The left-most column in Table 2 indicates the genotypes receiving the rewards (i.e. the 'player') whereas the top row represents the genotypes of the cells they are interacting with (i.e. the 'co-player'). Table 2 thus indicates that when two cells of Type A meet, each cell is rewarded with payoffs α. Similarly when two cells of Type B interact, each receives payoffs γ. An interesting event occurs when cells of different genotypes interact because the outcome can be asymmetric. In this case when a Type A and a Type B meet, the former is rewarded with β and the latter with δ. The expected payoff for an individual Type A cell is then

$$E_A = f_A\alpha + (1 - f_A)\beta, \tag{1}$$

and for a Type B

$$E_B = f_B\gamma + (1 - f_B)\delta. \tag{2}$$

If greater phenotypic payoffs in terms of proliferation as well as migratory activities correspond to higher fitness levels, then the average fitness of the entire tumor system

[3]Although we are aware of the 2D/3D distinction between cell migration and invasion, in here, we have used these two terms interchangeably to merely describe cell *motility*.

Table 2
Generic phenotypic payoff matrix of interactions between tumor cell genotypes A and B

		Encounter with	
		Type A genotype	Type B genotype
Payoffs to	Type A	α	β
	Type B	δ	γ

population can be computed as

$$E_T = \frac{2!(n-2)!}{n!}\left(\binom{n_A}{2}\alpha + n_A n_B(\beta+\gamma) + \binom{n_B}{2}\delta\right). \tag{3}$$

That is, the average fitness of the tumor system depends on the relative proportions of genotypes A and B in the total multicellular population of size n. Having derived this period's expected fitness, we can compute the next period's relative proportions of the existing genotypes in the population using the following difference equation:

$$f_{A,t+1} = f_{A,t}\frac{E_{A,t}}{E_{T,t}} \quad \text{and} \quad f_{B,t+1} = f_{B,t}\frac{E_{B,t}}{E_{T,t}}. \tag{4}$$

Eq. (4) shows that the population dynamics of the tumor system can be characterized by *path dependency*, i.e. the next period's genotypic composition depends on the current genotype composition, which in turn depends on the last period's genotypic composition, and so on. Depending on the particular parameter values, in the absence of spatial constraint this model has three alternative and stable outcomes: (i) **Coexistence.** Here, genotypes A and B coexist with stable proportions if $\delta > \alpha$ and $\beta > \gamma$. In this case, game theory predicts that cell population will consist of a roughly 50–50 stable mixture of both genotypes A and B cells. (ii) **Domination.** Type A will emerge as the sole dominant genotype if $\alpha > \delta$ and $\beta > \gamma$. That is, regardless of the population's genotypic composition, it always pays more to be a Type A. By contrast, Type B will dominate the cell population and drive Type A to extinction if $\delta > \alpha$ and $\gamma > \beta$. (iii) **Bistability.** If $\alpha > \delta$ yet $\gamma > \beta$, then either Type A or B vanishes depending on the initial mixture since cells fare best when matched with another cell of the same genotype.

It is important to realize that the payoff values above are only defined for every pair of cells. If we allow for the simultaneous interactions of more than two cells, then payoff values will depend on the genotypic composition in the cell's neighborhood. In these more general cases, the outcomes cannot be determined without recourse to numerical simulations. A simulation platform is also warranted if we want to consider explicitly the feedback effects between the tumor cells and their heterogeneous microenvironment. In that case, the cells' fitness levels depend not only on the genotypes of their peers, but also on environmental factors. This leads to a tumor system that evolves due to not only population dynamics but also the adaptive environment. Additionally, in the context of brain tumor growth in vivo, space serves as a key constraint because cell migration is limited locally (per unit of time) and cell–cell interactions (e.g. gap junctional communications, paracrine growth factor effects) are relatively short range. In that case, geography matters. To quantify the performance of an evolving tumor system that exhibits these three components—path dependency, dynamic feedbacks, and local interactions—a numerical model is required.

Different from the standard game-theory approach for tumor modeling that defines the payoffs only in terms of the promotion of a cell's proliferation activity, a novel feature of our numerical spatio-temporal model here is the notion of genetic differences defined not only in terms of (i) proliferative capability, but, in addition, also in terms of (ii) cell–cell communication and (iii) migratory capability (see Table 1). These genetic differences in turn translate into three categories of phenotypic payoffs: namely, in terms of gap–junction communication (GJC), proliferation activity, and migration activity.

Following Table 1, we assume that the highly proliferative Type A cells perform extensive GJC, inspired by in vivo experiments (Ghosh and Singh, 1997) showing that rapidly proliferating glioma cells (i.e., Type A cells here) exhibit a high density of gap–junctional channels. In this case, we define genetic differences in terms of distinct capabilities in GJCs conferring a certain degree of information processing within the tumor system. Simplified, GJC represent anatomical channels through the surface membrane that, if aligned, enable direct chemical signal transmission in between two neighboring cells (Kumar and Gilula, 1996).

To link cells' genotypes to their phenotypes, which in turn affect the tumor's fitness levels, we hypothesize that the extent of cell–cell GJ communication that depends on each cell's genotype affects its phenotypic behavior, i.e. whether a cell remains quiescent, proliferates, or migrates. Table 3 shows the phenotypic payoffs of cell–cell interactions in terms of GJC.

Specifically, according to Table 3, when a pair of cells interact within a spatially local neighborhood, the phenotypic payoffs in terms of the extent of cell–cell communication between these two cells becomes (i) very high (↑↑↑) if both cells are of Type A, (ii) high (↑↑) if Type A meets Type B, and (iii) normal (↑) if both cells are of Type B. In game-theoretic terms, the level of *cooperation* is highest among Type A cells.

Table 3
Gap junction (GJC) matrix specifies the phenotypic 'cell-cell communication' payoffs represented in a game-theory matrix format

Cell–cell communication payoffs	Type A genotype	Type B genotype
Type A	↑↑↑	↑↑
Type B	↑↑	↑

Table 4
The 'growth' payoffs measure the negative impact of gap–junction cell–cell interaction on the reproductive activities of the individual cells

Proliferation payoffs	Type A genotype	Type B genotype
Type A	↓↓↓	↓↓
Type B	↓↓	↓

The implications of these payoffs in terms of the cells' proliferation activities are as follows. As shown by the in vitro experiments of Zhu et al. (1992), lower proliferation activities correspond to a higher level of GJC. In particular, the authors show that overexpression of the GJC protein connexin 43 significantly *reduces* cell proliferation. Therefore, in Table 4 we link the extent of GJ communication to the (negative) payoffs of cell–cell interactions in terms of their phenotypic proliferation activities.

According to Table 4, since Type A cells exhibit the highest degree of intercellular coupling (see Table 3), the extent of this growth retardation is greatest when both cells are of Type A (↓↓↓), high when a Type A meets a Type B (↓↓), and limited when both cells are of Type B (↓). Note that even though a Type A cell experiences the highest reduction in proliferation activities when it interacts with its own type, we assume that the reduction is bounded from below such that Type A's proliferation activities (which are much higher than Type B's to begin with) never fall below those of Type B. Let π_i represent Type i's extent of proliferation activity for an isolated cell, and $\Delta\pi_{i,j}$ the negative payoffs in terms of the decline in proliferation activities when two cells of types i and j meet. Our boundary condition then guarantees that $\mathrm{Min}\,\pi'_A = \pi_A - \mathrm{Max}\,\Delta\pi_{A,i} > \pi_B$, $i = A, B$.

The aforementioned study focuses exclusively on proliferative activities. Glioma cells, however, also actively migrate and rapidly invade the surrounding brain parenchyma (Deisboeck et al., 2001). In a study that links GJC to the migratory behavior of glioma cells, McDonough et al. (1999) found that the fastest migrating cells are those expressing the *least* amount of connexin 43. Accordingly, Table 5 describes the extent to which GJ communication affects payoffs of cell–cell interactions in terms of their phenotypic migratory activity, thus linking Table 3 to cell migration activities.

Table 5
The 'migration' payoffs measure the inverse relationship between gap–junction cell–cell interaction and the migration activities of the individual cells

Migration payoffs	Type A genotype	Type B genotype
Type A	↑	↑↑
Type B	↑↑	↑↑↑

Specifically in Table 5, Type A cells exhibit the highest GJC (see Table 3); hence, the phenotypic migration payoffs are low when both cells are of Type A (↑), medium when a Type A meets a Type B (↑↑), and high when both cells are of Type B (↑↑↑).

3.2. Agent-based model

As stated earlier, our study here merges the aforementioned game-theory module with a previously-developed agent-based model (Mansury and Deisboeck, 2003, 2004), allowing the introduction of a heterogeneous population of tumor cells with distinct genotypes. Specifically, we link the genotype-dependent payoff values with the tumor cells' phenotypic activities of proliferation and migration. First, it is important to note the role of geography in our model: within each subpopulation (Type $i \in \{A, B\}$), cancer cells have identical genotypes, but can still exhibit different phenotypic behavior because of spatial modulations in the environmental conditions as well as a result of cell–cell interactions. As such, the model considers *both* genetic and epigenetic heterogeneity.

To focus on cell heterogeneity, our environmental factors consist only of nutrient supplies, while disregarding the impact of toxic metabolites and mechanical confinements, which we have elaborated in our previous works. Thus, there is no cell death linked to the accumulation of toxicity. Instead, here cells can perform one of these actions: proliferate, invade, or turn quiescent. In addition, we also assume here that both proliferation and migration occur within the same time scale as in our previous works. This simplification is due to the lack of experimental data detailing the precise time scales for different phenotypic behavior in the same setting.

For a tumor cell to either proliferate or migrate, its location must be on the tumor surface and at the same time satisfy minimum nutrient requirements reflecting the cell's metabolic demand. Specifically, the onset of both proliferation and migration must satisfy the threshold levels of nutrients, (ϕ_L, ϕ_U), such that a tumor cell in surface location ℓ proliferates if its onsite nutrient level exceeds the upper threshold, $\phi_\ell > \phi_U$, or

migrates to the surrounding parenchyma whenever $\phi_L < \phi_\ell < \phi_U$. Alive tumor cells that are trapped inside the tumor (hence are incapable of either proliferating or moving) or reside in locations with inadequate nutrients less than the lower threshold, $\phi_\ell < \phi_L$, enter a reversible, quiescent state.

3.2.1. Cell proliferation

The link between the game-theory module and the cells' proliferative activity is established the following way. We propose that the probability to proliferate for a Type i cell, $i \in \{A, B\}$, in location ℓ is determined in the following way:

$$Pr_{proliferate,j} = \phi_\ell / \left(\phi_\ell + k_{prolif,i}\right), i \in \{A, B\}, \quad (5)$$

where the parameter $k_{prolif,i}$ controls the extent of proliferation activity such that the higher its magnitude, the less likely proliferation can occur. Eq. (5) can be interpreted as the fitness generating functions of a Type i cell (Brown and Vincent, 1992), which specifies how an individual cell's proliferative activity relates to both the genotype of its neighbor (via $k_{prolif,i}, i \in \{A, B\}$) and the location-specific environmental factor (i.e. the onsite levels of nutrients ϕ_ℓ). As we have assumed in Table 1, Type A cells are highly proliferative genetically right from their origin (i.e., $k_{prolif,A} < k_{prolif,B}$). Because of the experimentally proven phenotypic dichotomy between growth and migration (Giese et al., 1996; Mariani et al., 2001) that is built into our agent-based algorithm, during their lifetime genetically more proliferative (and thus epigenetically, more proliferative active) Type A cells will also have lower probability (phenotypically) to migrate to the surrounding parenchyma. It is important to note here that in our model a cell with a specific genotype (either A or B) *over its lifetime* is capable of both proliferating and migrating, yet *at any given moment* if the cell is non-quiescent, then it can only either proliferate or migrate, but not both at the same time. For example, at time $t+1$ a cell that migrated in previous time t can certainly proliferate if certain environmental and spatial conditions are satisfied (see the Algorithm Implementation section below for specific details of these conditions), and vice versa.

In the absence of more specific experimental data, we assume for now a negative, linear link between the extent of GJ communication (Table 3) and phenotypic proliferation activities: $k'_{prolif,i} = \pi_{i,j} k_{prolif,i}$, $i,j \in \{A, B\}$. That is, the payoffs $\pi_{i,j}$ adjust downward the proliferative activity of a tumor cell whenever cell–cell interaction occurs. In particular, following Table 4, $\pi_{A,A} > \pi_{A,B} > \pi_{B,B}$ with $\pi_{A,B} = \pi_{B,A}$. For example, a Type A cell experiences the largest reduction in proliferative activities when it meets another Type A, whereas a Type B cell meeting a same-type cell experiences the least reduction. At any given time, however, a cell can interact with all its neighbors sharing a common border in the West, Northwest, North, Northeast, East, Southeast, South, and Southwest (i.e. the so-called 'Moore neighborhood'). When multiple interactions occur simultaneously, we assume a multiplicative rule:

$$k'_{prolif,i} = k_{prolif,i} \prod_j \pi_{i,j}, \quad (6)$$

where $i,j \in \{A, B\}$ and cell $j \in i$'s neighborhood.

3.2.2. Cell migration

Migrating cells compare the strength of chemical, diffusive signals that their local neighbors transmit. This modeling concept follows earlier works by Sander and Deisboeck (2002) arguing that 'homotype' attractor signals aid the emergence of branch-like migration patterns seen in experimental setups (Deisboeck et al., 2001). Such signals represent, e.g., the protein ligand TGF-α, which, after being secreted by the tumor cells themselves, acts paracrine in that it binds to the tumor cells' epidermal growth factor receptor. Specifically, the magnitude of the signal S_k that a cell k transmits from location ℓ at time t is a function of the current onsite level of nutrients, augmented by the signals transmitted by the cell's neighbors at time $t-1$:

$$S_k(t) = f[\phi_\ell(t)] + \sum_{m=0}^{n} w_m S_m(t-1), \quad (7)$$

where $m \in k$'s set of nearest neighbors and w_m denotes the distance-dependent weight. We define $f[\phi_\ell(t)] = 1 - 1/\phi_\ell(t)$, implying $\partial f / \partial \phi > 0$, i.e. higher nutrient levels amplify the magnitude of these paracrine signals, and hence guide the migration trajectory of tumor cells along the *chemotactic* path of 'highest attraction' (for this concept, see Deisboeck et al., 2001). We detail the numerical method calculating the signal weights in Eq. (11). Furthermore, we argue here that lower levels of GJ communication are associated with higher activities of migration phenotypically as mediated by the stronger signal S_k: $S'_k = \mu_{i,j} S_k$, $i,j \in \{A, B\}$, and $\mu_{i,j} > 1$. This inverse relationship follows McDonough et al. (1999), who argue that suppressing connexin-43 expression (i.e. lower GJ communication) allows glioma cells to detach from their neighbors, which in turn should accelerate migration. Following Table 5, we assume that $\mu_{B,B} > \mu_{A,B} > \mu_{A,A}$, i.e. a B–B interaction triggers cell motility through significant amplification, $\mu_{B,B}$, of the signal strength that guides migration. Note, however, that since we have the same time scale for both proliferation and migration in the current setting, this signal amplification mechanism has a lesser impact on B–B interactions than would be expected otherwise. Again a multiplicative rule prevails when a cell interacts with several local

neighbors simultaneously:

$$S'_k = S'_k \prod_j \mu_{i,j}, \tag{8}$$

where $i,j \in \{A,B\}$. An eligible cell m invades a neighboring location that transmits the strongest signal, art max S'_k, $k \in m$'s set of nearest neighbors.

3.2.3. Microenvironment

Finally, nutrient sources ϕ_ℓ evolve dynamically and spatially according to the following partial differential equation:

$$\frac{\partial \phi}{\partial t} = g_\phi \phi + \nabla \cdot (D_\phi \nabla \phi) - r_\phi n, \tag{9}$$

in which $\phi_\ell(t)$ stands for the nutrient levels at location ℓ and time t, $g_{\phi;}$ is the rate of nutrient replenishment, $D_{\phi;}$ the nutrient diffusion coefficient, $r_{\phi;}$ the rate of nutrient depletion, $n_\ell(t)$ the onsite population of tumor cells, and ∇ the spatial gradient operator. Biological examples for such extrinsic nutrient molecules include glucose and oxygen.

3.2.4. Surface roughness

We compute the roughness of the virtual tumor surface to track changes in the tumor's structural pattern. In this study here, surface roughness determines the variability of the tumor's diameter, measured as the distance between two opposing points on the tumor surface separated by a rotation of 180°. Extensive branching pattern imprinted mostly by migrating tumor cells thus should correspond to a higher degree of surface roughening. We compute surface roughness as the average squared deviations of the surface cell's distance from the average:

$$\langle s \rangle = \sum_{n=1}^{N_s} (d - \langle d \rangle)^2 / N_s, \tag{10}$$

where N_s denotes the number of cells occupying the tumor surface.

The following section details the algorithm implementation of our mathematical model.

4. Algorithm implementation

Here, our spatial framework is a 500×500 grid lattice corresponding to a 2D virtual brain tissue section. Initially, in that space we place two *replenished* nutrient sources (representing, e.g. cerebral blood vessels) at the grid center [i.e. at x–y coordinates (250,250)] and in the middle of the northeast (NE) quadrant [i.e. at (375,375)], respectively. We define Region 1 as the set of locations that is r_1 units of distance away from the grid center, $r_1 \le R_1$, and Region 2 as those r_2 units away from the middle of the NE quadrant, $r_2 \le R_2$, with $R_1 + R_2 = 125$. To establish a strong chemotactic gradient, the nutrient peak at Region 2 is set up to be 5 times higher than that at Region 1. As the simulation progresses, the nutrient level $\phi_\ell(t)$ at location ℓ and time t is updated according to Eq. (9). At the beginning of every simulation, we place 5 virtual cells of Type A and an equal number of Type B at the grid center. The current state of the virtual tumor cells at every step in the simulation is updated by the implementation of the following steps: (i) update paracrine-mediated cell signals, (ii) enable game-theory interactions, (iii) determine which cells proliferate, (iv) determine which cells migrate within the local neighborhood, and (v) determine which cells turn quiescent. Note that at any given time, a lattice site can be either empty or occupied by at most one single tumor cell. Also note that for a tumor cell to either proliferate or migrate, it must be located on the tumor surface; else it will turn quiescent (Freyer and Sutherland, 1986).

(i) *Update signal*: The strength of a tumor cell k's current signal S_k is calculated as a function of both the onsite nutrient levels and the weighted average of signals coming from the cell's neighboring locations. First, the distance weight w_m is calculated such that signals from nearby locations are assigned greater weights than those coming from distant locations:

$$w_m = 1.0 - \left(\frac{d_{k,m}}{d_{k,m} + r_S} \right), \tag{11}$$

where $m \in k$'s set of nearest neighbors, $d_{k,m}$ denotes the distance separating cells k and m, and r_S is a constant positive parameter. Having determined the weights w_k's, a cell's new signal for the next time period is calculated according to Eq. (7).

(ii) *Game-theory interactions*: The details of game-theory cell–cell interactions follow the descriptions specified above in the modeling section. As a result of these interactions, cells' proliferation parameter, $k_{prolif,i}$, and their signal strength, S_k, are adjusted based on the payoff matrices (see Tables 4 and 5).

(iii) *Determine cell proliferation*: A cell in location ℓ is allowed to proliferate if these conditions are met: (i) $\phi_\ell \ge \phi_U$ and (ii) there must be available locations for the new offspring to be placed adjacent to the parent cell (i.e. the parent cell must reside on the 'surface' of the tumor or cluster). If these conditions are met, then the tumor cell is allowed to proliferate with the probability determined by Eq. (5). Because proliferation is a probabilistic event, there will be a number of tumor cells that are eligible to proliferate but are not selected to do so at a given step.

(iv) *Determine cell migration*. A cell is allowed to migrate if (i) either it is eligible to proliferate but does not because of random chance, or its onsite

nutrient levels are lower yet sufficiently high to migrate: $\phi_L < \phi_\ell < \phi_U$, and (ii) there is at least one unoccupied, adjacent location for the cell to invade that is one lattice site away. If these criteria are met, then an eligible tumor cell migrates and follows the direction of the strongest signal, S_k, as defined in Eq. (7).

(v) *Determine cell quiescence*. Cells that do not proliferate or migrate automatically enter a reversible, quiescent state.

5. Results

In the following, we show results from varying the payoffs for A–A cell–cell interactions in terms of their phenotypic proliferative activities (see Table 4). Recall from our modeling section that interactions between a pair of A–A cells result in the steepest reduction of the proliferation activity for both cells involved. We have also experimented with various migration payoffs for B–B interactions, yet as expected we did not find a discernible pattern in their spatio-temporal performance due to our current setup of equal time-scale for both proliferation and migration, which implies that during either proliferation or migration, the tumor expands to a vacant lattice site that is one unit of distance away from the parent's location for the former or the migrating cell's original location for the latter.

5.1. Average velocity

Here, average velocity serves as a measure for the tumor's overall performance. Fig. 1 shows that as on the

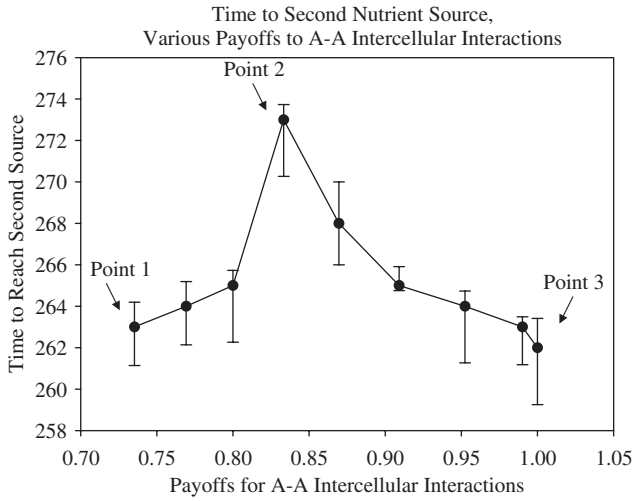

Fig. 1. Plot of the time to the second nutrient source (i.e. the inverse of the tumor's average velocity) versus various payoff values conferred to A–A intercellular interaction. The error bars indicate the standard deviations from performing 10 Monte Carlo simulations for each value of payoffs for A–A interactions.

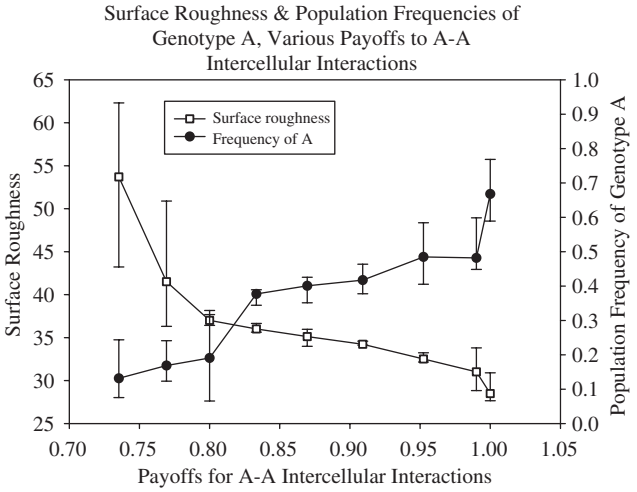

Fig. 2. Plot of various payoff values conferred to A–A intercellular interaction versus surface roughness (*open squares*, left *y*-axis) and frequency of genotype A in the population (*closed circles*, right *y*-axis). The error bars indicate the standard deviations from performing 10 Monte Carlo simulations for each payoff value conferred to A–A interactions.

x-axis the payoffs conferred to A–A interaction increase in terms of lesser reduction of Type A's proliferative activities, unexpectedly the average velocity of the tumor's spatial expansion exhibits a *phase transition.* That is, initially the time to the second nutrient source rises, representing declining velocity, as the A–A payoffs increase. But then it appears to reach a minimum velocity at a payoff of approximately 0.83 before it rises again, as Type A cells become the numerically dominating genotype (see the right *y*-axis in Fig. 2) in the total population (i.e. including proliferating, migrating, and quiescent cancer cells) at a payoff of 1.00.

5.2. Structural patterns and genotypic robustness

Fig. 2 shows that as the payoffs conferred to A–A cell–cell interaction increase, surface roughness declines continuously (left *y*-axis). At the same time, the frequency of genotype A (right *y*-axis) in the total population increases monotonically, i.e. becomes more robust. That is, as the more proliferative yet less migratory Type A becomes dominant, surface roughness declines. Conversely, surface roughness rises as the more migratory Type B becomes the dominating genotype (at lower A–A payoffs), consistent with our previous study examining 'structural–pattern' relationship (Mansury and Deisboeck, 2004) showing a positive correlation between fractal dimensions of the tumor surface and the number of migrating cells.

5.3. Time series and spatial profile of tumor genotypes

To better understand the evolution of the tumor cells over time, here we examine the time series of

migrating and proliferating cells broken down by genotypes. Figs. 3(a)–(c) show the results from varying the payoffs conferred to A–A interactions. In Fig. 3(a), when the A–A payoffs are low (= 0.73, i.e. *large* reduction in proliferation activity of A cells), as expected genotype B dominates both migration and proliferation over time and across regions. Note that these results correspond to "Point 1" in Fig. 1, where the tumor's velocity is relatively high (i.e. lesser time to reach source 2).

When the A–A payoffs rise to 0.83 (i.e. *smaller* reduction in proliferative activity, Fig. 3(b)), as expected genotype A now starts to dominate both migration and proliferation. An *oscillating* pattern emerges here for the time series of proliferating cells, with initially increasing dominance of genotype A just before the tumor crosses the border between Regions 1 and 2. However, as the tumor crosses the border of Region 2 (at $t = 157$), the proportion of genotype A decreases, reaching a 50–50 composition as it approaches the center of source 2. Fig. 3(b) thus shows that the dominant genotype can change based on alterations in the environmental conditions, in this case the rising supplies of nutrient in Region 2 that is up to 5 times higher than in Region 1. Note that A–A payoffs = 0.83 corresponds to the slowest velocity of the tumor's spatial expansion, i.e. 'Point 2' in Fig. 1.

Finally, increasing the A–A payoffs further to 1.00 (Fig. 3(c)) leads to a diametrically opposite and rather unexpected result, namely genotype B returns to completely dominate the composition of both migrating and proliferating cells, despite genotype A dominating the total population (see Fig. 2). Thus, at high A–A payoffs, Type A numerically dominates the entire cell population; however, the majority of this genotype comprises *quiescent* cells (data not shown here), which leads to Type B dominating both proliferation and migration activities. These results correspond to 'Point 3' in Fig. 1, where the tumor's velocity is again relatively high.

6. Discussion

Here, we have integrated a game-theory module into our previously developed agent-based model of 'monoclonal' brain tumors (Mansury and Deisboeck, 2003, 2004). This game-theory module not only specifies the impact of intercellular communications but also extends the agent-based framework to the more realistic case of

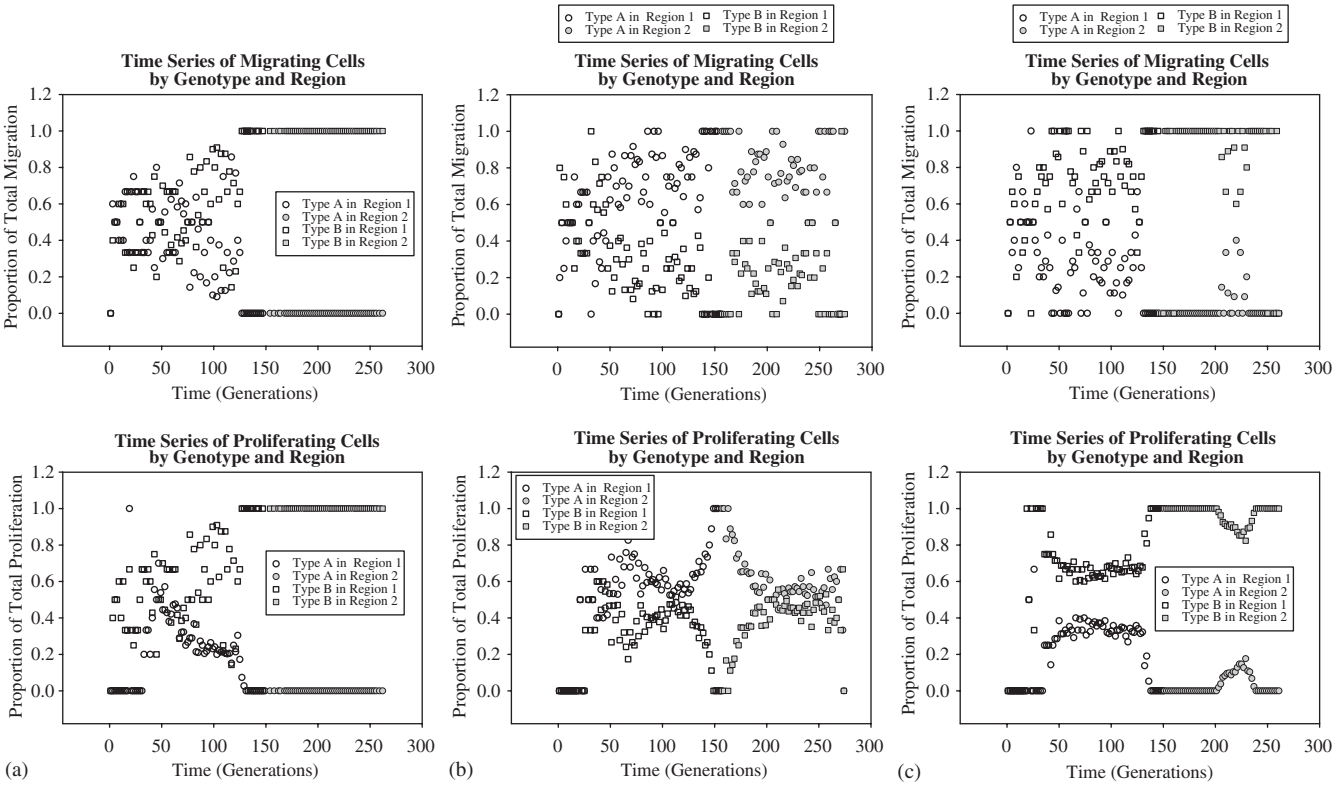

Fig. 3. Time series of a number of tumor cells for various payoff values conferred to A–A interactions. (a) A–A payoffs = 0.73, (b) A–A payoffs = 0.83, (c) A–A payoffs = 1.00. The top figures show the time series of migrating cells broken down by genotypes as a proportion of total migration, while bottom figures represent the time series of proliferating cells broken down by genotypes as a proportion of total proliferation. *Open circles* represent Type A cells in Region 1, *closed circles* in Region 2. *Open squares* represent Type B cells in Region 1, *closed squares* in Region 2.

polyclonal tumor cell populations. Among such heterogeneous cell populations, competitive selection pressure favors the 'fittest' clone. To simplify our analysis, as a starting point we assume that the tumor population consists of two static genotypes A and B, although we are aware that in reality new cancer genotypes continuously evolve over time. Having established a simulation platform here, in future works we can allow the emergence of new subpopulations through either e.g. mutation.

What is not clear a priori is whether higher fitness, in this case measured as spatio-temporal expansion velocity, corresponds to the more proliferative genotype A or to the more migratory genotype B. To establish the link between the tumor fitness and genotypes, we examined the impact of changing the A–A payoffs on the tumor's average velocity. These payoffs affect the phenotypic behavior of the A cells, yet the values of these payoffs depend on the genotypes of the interacting cells.

With regard to the overall performance of the tumor, we found a phase transition in the average velocity of the tumor's spatiotemporal expansion. That is, velocity initially falls as the payoffs to A–A interactions increase, but rises again when the payoffs increase further. This phase transition is rather surprising because at the individual cellular level, Type A cells are highly proliferative yet less migratory, and thus without running the simulations one would expect the velocity to decline continuously as the stationary Type A becomes the dominating genotype in the total population, on the numerical expense of the spatially more aggressive, highly migratory Type B clone.

On the structural side, we found that surface roughness increases as the A–A payoffs decrease, accompanying a monotone decrease of the genotype A cells in the total population (i.e. including proliferating, migrating, and quiescent cells, in all regions). Taking Figs. 1 and 2 together, one can therefore conclude that lesser A–A phenotypic payoffs (Table 4) expectedly (i.e. due to spatial competition) promote a higher frequency of the more migratory Type B, which in turn leads to both the roughening of the tumor's surface through largely migratory cell branches and, consequently, an accelerating spatio-temporal expansion. Point 1 in Fig. 1 thus represents a 'migration'-driven velocity optimum and the corresponding time series indeed confirms that at low A–A payoffs, genotype B is the dominant tumor cell clone in both Regions 1 and 2.

Now, as the A–A payoffs rise further, as expected the more proliferative Type A increases its population frequency and becomes the dominating clone in both migration and proliferation. Hence, Fig. 1's Point 2 corresponds to a 'proliferation'-driven spatial expansion, resulting in both fewer migratory cell branches and thus an overall smoother tumor surface. Interestingly, this intermediate value of A–A payoffs associated with the lowest average velocity corresponds to a 50–50 *coexisting*, bi-clonal population where neither genotype dominates. In terms of Eq. (3), if we accept the notion that a higher competitive advantage of the tumor and thus its fitness is associated with faster spatial expansion into the surrounding environment, then E_T (i.e. the tumor's overall fitness) is a direct and positive function of the tumor's average velocity. In this particular setting, clonal coexistence thus yields a competitive disadvantage in terms of spatial aggression. However, one can expect this to change once therapeutic impact comes to play, where a more heterogeneous tumor cell composition should prove to confer a distinct competitive benefit.

Finally, as the A–A payoffs increase even further, genotype B again returns to lead both migration and proliferation and that is despite the fact that genotype A dominates the total population composition (right y-axis of Fig. 2). The result is a relatively high average velocity (Point 3 in Fig. 1), yet, intriguingly, accompanied by a lesser extent of surface roughening. As this point of high A–A payoffs fosters more Type A cells and (again, due to spatial competition) concomitantly less of Type B, the number of Type B cells in the total population per se does not appear to be as crucial for the overall tumor dynamics as their number among actively proliferating and migrating cells (Figs. 3a and c). One can argue that the rapid transition of proliferative to quiescent stage accounts for the relative increase of Type A in the total population while ensuring a relative increase in Type B among actively proliferative and migratory cells. Thus, *less* Type B cells in the total cancer cell population gain *more* importance for the overall tumor behavior. Surface roughening does not occur as extensively, precisely because of the lesser proportion of the spatially more aggressive Type B cells in the overall population.

Even at this early stage, our results already may have potentially useful implications for cancer research. For instance, the finding that environmental, i.e. anatomical, conditions can effectively alter the dominant genotype or clone within a heterogeneous population is both intriguing and instructive, as this seems to confirm the need for a geographic array of tissue biopsies, rather than rely on a single one, in order to achieve reasonable predictive power for the behavior of the entire neoplasm. Secondly, one would expect a Type A-dominated highly proliferative tumor cell population to lead to a *lower* malignant tumor with reduced migratory ability. However, as our results show, spatially highly aggressive malignant behavior can emerge unexpectedly from a Type A-dominated heterogeneous cancer cell population as well. In other words, that more invasiveness sustains a more aggressive tumor growth pattern is commonly accepted; however, that under some circumstances a smaller number of migratory cells (in the total

population) can come to dominate the tumor's emergent dynamics, potentially without even causing noticeable structural changes, is rather alarming given that cancerous structures need to reach a certain size to become detectable on image, a prerequisite for image-guided biopsies in clinics.

In a future work, we plan among other extensions to specify different time scales along with allowing more than one cell per lattice site for proliferation and migration, thus allowing B–B migration payoffs to generate distinct spatiotemporal patterns. Adding mutational events in order to trigger progressive changes of the currently static genotypes will render the framework biologically more realistic and should provide a starting point to explore the coupling between proliferation capabilities and mutation rates for glioma cells, as Sasaki and Nowak (2003) have done for the general theoretical case. Another potential extension would be to include other environmental variables, such as toxic metabolites and mechanical confinements, and to examine the impact of the former on cell death and the latter on varying cell densities.

In summary, this model and its future iterations should prove useful in our effort to better understand the underlying mechanisms of tumorigenesis based on the genotypic–phenotypic link, and thus support the claim that game theory approaches will soon gain an essential role in interdisciplinary cancer research.

Acknowledgments

This work has been supported by Grants CA 085139 and CA 113004 from the National Institutes of Health and by the Harvard-MIT (HST) Athinoula A. Martinos Center for Biomedical Imaging and the Department of Radiology at Massachusetts General Hospital. Y.M. is the recipient of an NCI-Training Grant Fellowship from the National Institutes of Health (CA 09502).

References

Bach, L.A., Bentzen, S.M., Alsner, J., Christiansen, F.B., 2001. An evolutionary-game model of tumour–cell interactions: possible relevance to gene therapy. Eur. J. Cancer 37, 2116–2120.

Brown, J.S., Vincent, T.L., 1992. Organization of predator–prey communities as an evolutionary game. Evolution 46, 1269–1283.

Deisboeck, T.S., Berens, M.E., Kansal, A.R., Torquato, S., Stemmer-Rachamimov, A.O., Chiocca, E.A., 2001. Pattern of self-organization in tumor systems: complex growth dynamics in a novel brain tumor spheroid model. Cell Prolif 34, 115–134.

Dugatkin, L.A., Reeve, H.K., 1998. Game Theory and Animal Behavior, Eds. Oxford University Press, Oxford.

Freyer, J.P., Sutherland, R.M., 1986. Regulation of growth saturation and development of necrosis in EMT6/Ro multicellular spheroids by the glucose and oxygen supply. Cancer Res 46, 3504–3512.

Gatenby, R.A., Gawlinski, E.T., 1996. A reaction–diffusion model of cancer invasion. Cancer Res 56, 5745–5753.

Gatenby, R.A., Vincent, T.L., 2003a. An evolutionary model of carcinogenesis. Cancer Res 63, 6212–6220.

Gatenby, R.A., Vincent, T.L., 2003b. Application of quantitative models from population biology and evolutionary game theory to tumor therapeutic strategies. Mol. Cancer Ther. 2 (9), 919–927.

Ghosh, P., Singh, U.N., 1997. Intercellular communication in rapidly proliferating and differentiated C6 glioma cells in culture. Cell Biol. Int. 21 (9), 551–557.

Giese, A., Loo, M.A., Tran, N., Haskett, D., Coons, S., Berens, M.E., 1996. Dichotomy of astrocytoma migration and proliferation. Int. J. Cancer 67, 275–282.

Gonzalez-Garcia, I., Sole, R.V., Costa, J., 2002. Metapopulation dynamics and spatial heterogeneity in cancer. Proc. Natl Acad. Sci. USA 20, 13085–13089.

Hamilton, W.D., 1967. Extraordinary sex ratios. Science 156, 477–488.

Kansal, A.R., Torquato, S., Chiocca, E.A., Deisboeck, T.S., 2001. Emergence of a subpopulation in a computational model of tumor growth. J. Theor. Biol. 207 (3), 431–441.

Kumar, N.M., Gilula, N.B., 1996. The gap junction communication channel. Cell 84, 381–388.

Mansury, Y., Deisboeck, T.S., 2003. The impact of 'search-precision' in an agent-based tumor model. J. Theor. Biol. 224, 325–337.

Mansury, Y., Deisboeck, T.S., 2004. Simulating 'structure–function' patterns of malignant brain tumors. Physica A 331, 219–232.

Mariani, L., Beaudry, C., McDonough, W.S., Hoelzinger, D.B., Demuth, T., Ross, K.R., Berens, T., Coons, S.W., Watts, G., Trent, J.M., Wei, J.S., Giese, A., Berens, M.E., 2001. Glioma cell motility is associated with reduced transcription of proapoptotic and proliferation genes: a cDNA microarray analysis. Neurooncology 53, 161–176.

McDonough, W.S., Johansson, A., Joffee, H., Giese, A., Berens, M.E., 1999. Gap junction intercellular communication in gliomas is inversely related to cell motility. Int. J. Dev. Neurosci. 17 (5-6), 601–611.

Nowak, M.A., May, R.M., 1995. Evolutionary games and chaos. Nature 359, 826–829.

Nowak, M.A., Sigmund, K., 1989. Oscillation in the evolution of reciprocity. J. Theor. Biol. 137, 21–26.

Nowak, M.A., Sigmund, K., 2004. Evolutionary dynamics of biological games. Science 303, 793–799.

Roskelley, C.D., Bissel, M.J., 2002. The dominance of the microenvironment in breast and ovarian cancer. Semin. Cancer Biol. 12, 97–104.

Sander, L.M., Deisboeck, T.S., 2002. Growth patterns of microscopic brain tumors. Phys. Rev. E 66, 051901.

Sasaki, A., Nowak, M.A., 2003. Mutation landscapes. J. Theor. Biol. 224, 241–247.

Shapiro, J.R., 1986. Biology of gliomas: heterogeneity, oncogenes, growth factors. Semin. Oncol. 13, 4–15.

Smith, J.M., Price, G.R., 1973. The logic of animal conflict. Nature 246, 15–18.

Sole, R.V., Bascompte, J., 1992. Stability and complexity in spatially-extended two-species competition. J. Theor. Biol. 159, 469–480.

Tomlinson, I.P.M., 1997. Game–theory interactions between tumour cells. Eur. J. Cancer 33, 1495–1500.

Tomlinson, I.P.M., Bodmer, W.F., 1997. Modelling the consequences of interactions between tumour cells. Brit. J. Cancer 75, 157–160.

Zhu, D., Kidder, G.M., Caveney, S., Naus, C.C., 1992. Growth retardation in glioma cells cocultured with cells overexpressing a gap junction protein. Proc. Natl Acad. Sci. USA. 89 (21), 10218–10221.